

## Influence of Nozzle Diameter on Spray Characteristics and Surface Heat Transfer Dynamics in Cryogen Spray Cooling for Dermatologic Laser Surgery

Zhifu Zhou<sup>1</sup>, Rui Wang<sup>1</sup>, Guoxiang Wang<sup>1,2\*</sup>, Bin Chen<sup>1\*</sup>

<sup>1</sup>State Key Laboratory of Multiphase Flow in Power Engineering,  
Xi'an Jiaotong University, Xi'an, 710049, China

<sup>2</sup>Department of Mechanical Engineering, University of Akron, Akron, OH 44325, USA  
\*chenbin@mail.xjtu.edu.cn and gwang@uakron.edu

### Abstract

Cryogen spray cooling (CSC) is an effective method to minimize or even eliminate laser-induced irreversible injury to the epidermis during laser surgery of various cutaneous anomalies such as port wine stain (PWS). This paper conducts an experimental investigation of the atomization characteristics and surface heat transfer dynamics in pulsed cryogen spray cooling of epidermis by R-134a, focusing on the effect of the nozzle diameter. A Phase Doppler Particle Analyzer (PDPA) is used to measure the distributions of the diameter and velocity of the liquid droplets in the spray. The temperature of liquid droplets in spray is measured by a micro-thermocouple with a bead diameter of around 100  $\mu\text{m}$ . A thin-film thermocouple of 2  $\mu\text{m}$  thickness is deposited directly onto the epoxy resin substrate (which serves as the skin phantom) to monitor the variation of the surface temperature induced by the CSC. The dynamic variation of the surface heat flux and convective heat transfer coefficient in CSC can then be quantified from the measured temperatures using the Duhamel's theorem. Four nozzles with diameter ranging from 0.48 mm to 1.75 mm have been used and a systematic parametric study was conducted to illustrate the effect of nozzle diameter on spray characters and surface heat transfer dynamics. It is found that the nozzle with the smaller diameter produces finer liquid droplets and larger droplets velocity than that with the larger diameter. Furthermore, the temperature of droplets from the smaller diameter nozzle decreases faster with the spray distance. Analysis of surface heat transfer indicates that the size and velocity of liquid droplets in spray has a large effect on surface heat flux and heat transfer coefficient, with large droplets leading to high heat flux at the cooling surface. In addition, a criterion is proposed to evaluate the cooling efficiency of a given nozzle based on the variation of heat extraction from the cooling surface within the effective cooling time. These results can be used to guide the selection of nozzles during cryogen spray cooling for laser dermatology.

---

### 1. Introduction

Port wine stain (PWS) is one kind of congenital vascular birthmarks in the dermis that occur in approximately 0.3% to 0.5% of infants. Initially, it appears as flat, pink to red patches that may progressively be darken and thicken with age [1]. PWS mostly happens on body's exposed places, such as head and neck, which may significantly impede the patients' psychosocial development and well-being [2]. Recently, the Pulsed Dye Laser (PDL) of wavelengths at 585 nm or 595 nm is the most common choice for the treatment of PWS, following the principle of selective photothermolysis [3]. The objective is to cause selective thermal damage to subsurface targets (chromophores such as blood vessels) without causing damage to the overlying normal tissues (e.g. epidermis). However, the absorption of laser energy by the melanin in epidermis not only reduces the therapeutic outcomes but also causes irreversible thermal damage to skin [4]. Cryogen spray cooling (CSC) is therefore used to precool selectively the superficial layer of skin to minimize or even eliminate laser-induced irreversible injury to the epidermis [5]. The standard refrigerant currently used in the clinical laser surgery is R-134a, which can make the skin surface temperature drop above 40 °C within very short time (tens of milliseconds) after it is released through the straight-tube nozzle. The effective cold protection to the epidermis by CSC has inspired lots of studies on this unique spray in the last twenty years, but mainly focused on the surface heat transfer dynamics. Aguilar et al. [6] firstly used a copper rod as the spray object to study the heat flux ( $q$ ) and heat transfer coefficient ( $h$ ) produced by the straight-tube nozzles with two diameters (0.7 mm and 1.4 mm) under the steady spray. They found that the large diameter nozzle could produce much higher  $q$  and  $h$ . Then cryogen was sprayed on the upper surface of a thin silver disk (10.48 mm diameter and 0.42 mm thickness) with a type-K thermocouple (300  $\mu\text{m}$  bead diameter) attached to its lower surface to study  $q$  and  $h$  of two commercial nozzles (with diameter 0.5 mm and 0.8 mm) under pulsed spray [7]. Similarly, they found that large diameter nozzle produced the higher maximum heat transfer coefficient ( $h_{max}$ ). In this study, they also investigated the variations of droplet diameter and velocity by the PDPA. The results showed that the smaller diameter nozzle produced a better atomization. More recently, they developed a fast response surface temperature measurement method to monitor the fast temperature variation of pulsed spray which consisted of a thin (30  $\mu\text{m}$ ) aluminum foil attached to a small thermo-

couple (50  $\mu\text{m}$ ) on the lower surface and exposed to the cryogen spurt on the upper surface [8]. Based on this method, the effect of spray angle [9], spray distance [10] and spurt duration [11] on the surface heat transfer dynamics was studied. Their results showed that the spray angle and the spurt duration had insignificant impact on the surface heat transfer dynamics while the spray distance was the major factor. Brain et al. [12] utilized four types of delivery devices to investigate the effects of droplet size and spray density on the heat removal from the skin phantom (Epoxy resin). They found that the variation of heat removal by various delivery devices was modest in spite of the relatively large differences in cryogen mass output and droplet size.

From the literatures mentioned above, one can see that lots of efforts have been conducted to study the surface heat transfer dynamics induced by CSC and to optimize the nozzle design. Nevertheless, the most recent review paper finds that a large population of patients with PWS responds poorly to laser treatment, with a range of 12% to 80% of patients achieving less than 50% clearance [13]. Therefore, there is still necessary to develop the treatment strategies and to enhance the cooling efficiency. This paper presents an experimental investigation of the atomization characteristics and surface heat transfer dynamics in pulsed cryogen spray cooling of R-134a, focusing on the effect of the nozzle diameter since the length of the nozzle has little impact on the surface heat transfer [6, 14]. Four straight-tube nozzles which resemble those used in the commercial devices with diameter ranging from 0.48 mm to 1.75 mm have been used in the experiments to measure the distributions of the diameter and velocity of the liquid droplets in the spray. After the measurement of temperature of liquid droplets and the epoxy resin substrate (which serves as the skin phantom), the dynamic variation of the surface heat flux and convective heat transfer coefficient in CSC can then be quantified from the measured temperatures through Duhamel's theorem. The effect of the spray distance on the spray characteristics and surface heat transfer dynamics is also investigated. In addition, a criterion is proposed for the guidance of selection of nozzles for the use of CSC.

## 2. Experimental System and Numerical Methods

### 2.1. Spray setup

Fig.1 is the schematic of the experimental system. It consists of a pressure vessel for storage of cryogen, a three-dimensional translational electric position stage (WN105TA300M by Beijing Winner Optics Instruments Co., China) with space resolution of 8  $\mu\text{m}$ , a solenoid electric valve (B2021SBTTO24DVC by Gems, USA) that can open or close within 5 ms, and four straight-tube nozzles. The geometry of the nozzle resembles that of the commercial nozzles used for cryogen spray cooling in the laser surgeries, which is made of a stainless steel tube with the same length of 40 mm and different diameters of 0.48 mm, 0.96 mm, 1.21 mm and 1.75 mm, respectively. The vessel is a commercial R-134a (Dupont) cryogen container and is pressurized at the saturation pressure of this cryogen at room temperature (0.67 MPa at 25  $^{\circ}\text{C}$ ). The Valve is installed in the position stage, which controlled by the computer can exactly adjust the position of the nozzle in three dimension. The nozzle fits tightly into the opening of the solenoid valve. A standard high-pressure hose connects the cryogen vessel to the valve. A micro-scale flowmeter (931-06xx by Gems, US) is located in the middle of the high-pressure hose to monitor the flow rate of the spray.

### 2.2. Droplet Size and Velocity Measurement

A phase Doppler Particle Analyzer (PDPA by TSI, USA) is used to measure the velocities including the axial and radial directions and diameter of the droplets in the cryogen spray of-R134a. The PDPA generates four interfacing laser beams of different wavelengths, which focus on a probe volume, typically smaller than  $1\text{mm}^3$ . When droplets go through the probe volume, these beams are interfaced and a Doppler signal with a frequency shift proportional to the droplet velocity is generated. The phase difference between the signals collected by adjacent detectors is proportional to droplet diameter. Before taking the measurements, the optimum values of the PDPA parameters had to be selected including the diameter range, velocity range and the laser power. For each measurement, the spray duration lasts 10 seconds. In this study, we chose the Sauter mean diameter ( $D_{32}$ ) and the arithmetic mean axial velocity ( $U$ ) as the average droplet diameter and velocity.

### 2.3. Temperature Measurements

A standard type-T thermocouple (Omega, USA) with bead diameter of 100  $\mu\text{m}$  is placed to the spray to measure the average temperature of cryogen in spray along the central axis. Since the estimated response time of the thermocouple is fairly long, about 10ms, only a steady state cryogen temperature of spray is obtained.

A thin film thermocouple (TFTC) of type-T of two microns in thickness is deposited directly on the epoxy substrate (50 mm  $\times$  50 mm  $\times$  5 mm) to monitor rapid change of the surface temperature during a pulsed spray. The reason for choosing epoxy resin as the cooling substrate is that its thermal property likes that of human skin [12, 15]. The response time of TFTC is about 1.2  $\mu\text{s}$ , which is fast enough to measure the rapid change of the surface temperature [16]. So the TFTC sensor indeed provides 'real-time' surface temperature measurements. For detail information of the method of surface temperature measurement using TFTC, please refer to our previous job reported in the literature [16].

For surface temperature measurements in pulse spray, both the solenoid valve and the thermocouple are connected to the computer and controlled through a Labview control system. The thermocouple measurements is

acquired at 100 kHz and converted to the temperature data using a DAQ board (NI: M-6251). During experiments, the spray duration is firstly set in the Labview controlling panel. When the valve is turned on, the temperature data from TFTC is acquired simultaneously.

Separate cases have to be carried out to make the PDPA and temperature measurements. The volume flow rates of liquid R-134a under the steady spray are 0.21 ml/s, 3.39 ml/s, 5.69 ml/s and 11.48 ml/s respectively, from the minimum diameter nozzle to the maximum diameter nozzle through the micro-scale flowmeter experimental results. The relative error is less than 2% with our calibration using water. In order to save the consumption of the refrigerant, the PDPA measurement in the section 3.1 didn't include the maximum diameter nozzle ( $d_N=1.75$  mm) since the spurt duration for PDPA measurement should be long enough (10 s). For all the experiments, the room temperature was kept at about 25 °C, and the relative humidity was about 20%.

#### 2.4. Heat Transfer Calculations

The surface temperature measured by TFTC can be seen as the real surface temperature since it is directly deposited on the substrate surface with the depth of only 2  $\mu\text{m}$ . Then the Duhamel's theorem can be used to evaluate the temperature gradient at the substrate surface and get the surface heat flux with the assumption of one-dimensional heat transfer problem along the depth direction. Franco et al. [17] and Zhou et al. [18] have given a detailed description of solving this problem using Duhamel's theorem, and the heat flux equation is given as equation (1).

$$q(t) = \sqrt{\frac{\kappa\rho c}{\pi}} \int_{t_o}^t \frac{1}{\sqrt{t-\tau}} \frac{dT}{d\tau} d\tau \quad (1)$$

Where  $q$  is the surface heat flux,  $\kappa$ ,  $\rho$ ,  $c$  are the heat conductivity, density and specific heatcapacity, respectively.  $T$  is the temperature,  $t_o$  and  $t$  are the initial time and the terminate time at the time step  $\tau$ . Once known  $q$ , the surface heat transfer coefficient can be calculated by the following equation,

$$h(t) = \frac{q(t)}{T_d - T_s} \quad (2)$$

Where  $h$  is the heat transfer coefficient,  $T_d$  and  $T_s$  are the temperature of spray droplets and surface of the cooling substrate at the given spray distance.

### 3. Results and Discussion

#### 3.1. Droplet density, diameter and velocity

The spray characteristics of the nozzles are shown in the term of the variations of centerline droplets number, diameter, velocity and temperature with the spray axial distance. We firstly examine the variation of the centerline droplets number by PDPA measurement along the spray axial distance for different diameter nozzles except the maximum diameter nozzle,  $d_N=1.75$  mm (and this is the same as the following for the show of droplet diameter and velocity). To ensure the statistic meaning of the results, the droplets number detected by PDPA should be large enough. For each point measurement, the spurt duration is 10 s. It's can be seen that the droplets numbers at most of the measured points are more than 5,000, except for the points that are very near the exit of the nozzles. The droplets number firstly increases with the increment of the spray distance until reaching the maximum value at different places for different nozzles. Generally, the smaller the nozzle diameter is, the closer the point where the maximum value emerges is from the nozzle exit. If we define the distance between the nozzle exit to this point is the best atomized distance, it can be noticed that the smaller diameter nozzle has the shorter best atomized distance. Additionally, Fig.2 shows that all the variations of centerline droplets number with the axial spray distance present the Gaussian shape.

Fig.3 illustrates the droplets number variations with the dimensionless spray axial distance normalized by the droplet diameter ( $d_N$ ). It can be found that all of number points can be linearly fitted using the Gaussian distribution function. The non-dimensional best atomized distance for all the nozzles is about 100.

Fig.4 presents the variation of the centerline average droplet diameter ( $D_{32}$ ) with the axial distance for different diameter nozzles, which shows quick reduction in the average droplet diameters in the first 50 mm of the spray for all the nozzles, and this observation has also been made by Yildiz et al. [19]. One explanation of such a quick reduction in the droplet size is related to the atomization mechanism of superheated cryogen out of the nozzle. The high temperature liquid droplets out of the nozzle found themselves in a superheated state and would be explosively atomized quickly into smaller droplets to reduce the non-equilibrium driving force. After the quick reduction, there is only very small change in the average droplet diameter in the later spray region. It's noticed that the small diameter nozzle produces smaller average droplet diameter at all the measured points. This means the small diameter nozzle has the better atomized capacity than that of the large one. Comparing our experimental droplet diameter data with those by others using the same R-134a, it can be found that our data is comparable with those by Vu et al. [20], while is much smaller than those by Yildiz et al. [19]. The large differ-

ence may attribute to the difference of the nozzle diameter used in the spray, as the nozzle diameter is 5 mm in Yildiz's study, which is much larger than those by Vu et al. [20] and us.

Fig.5 shows the variation of the average droplet axial velocity ( $U$ ) on the centerline with the axial distance for different diameter nozzles. Contrary to the variation of  $D_{32}$ ,  $U$  firstly experiences an acceleration process until reaching the maximum value at the distance of about 30 mm. This acceleration is also observed by Aguilar et al. [7], Vu et al. [19] and Yildiz et al. [20], which can be explained by the unique superheated atomization mechanism. Then  $U$  decreases rapidly with increasing the spray distance due to the drag force acting on the droplets by the surrounding gas. Similarly with  $D_{32}$ , large diameter nozzle produces large  $U$  at all the measured point, which suggests that the droplets from the large diameter nozzle has a greater impact on the cooling surface at the same distance.

### 3.2. Droplet temperature in spray

The variation of average droplet temperature ( $T_d$ ) in the spray with the spray distance is shown in Fig. 6. The details of how this temperature obtained can be found in our previous work [21]. The centerline temperature initially shows an almost exponential decay [22], with the fastest drop taking place near the nozzle exit for all the nozzles. The temperature drop slows down as spray develops further for the rapid evaporation of droplets and the insufficiency of the convective heat transfer from the surrounding. Eventually, the centerline temperature reaches a minimum value ( $T_{d,min}$ ) of  $-60 \pm 1$  °C for the four nozzles at different places. After reaching  $T_{d,min}$ , one sees a sudden large increase in the centerline temperature due to the continuous heating acting on the droplets by the ambient gas. Inspecting the temperature variations for different diameter nozzles, it can be found that the droplet temperature from the nozzle decreases faster and  $T_{d,min}$  emerges earlier with the smaller diameter, which strongly indicates one should keep cautious to control the spray suitable distance as they use different diameter nozzles in CSC.

We normalize the droplet temperature for all the nozzles before it rise up in terms of  $(T_d - T_{d,min}) / (T_{sat} - T_{d,min})$  as the function of the non-dimensional axial distance ( $z/d_N$ ), where  $T_{d,min}$  and  $T_{sat}$  are the droplet minimum temperature (-60 °C) and saturated temperature at the atmospheric pressure, see Fig. 7. An interesting feature can be found that all the temperature points show self-similar profile, which can be correlated by an exponential equation, as given in equation (3).

$$\frac{T_d - T_{d,min}}{T_{sat} - T_{d,min}} = \exp(-0.025 \frac{z}{d}) \quad (3)$$

### 3.3. Surface heat transfer dynamics of pulsed spray cooling

Since the spray distance has significant effect on the dynamics of surface heat transfer in CSC [10], the surface heat transfer behavior of different diameter nozzles under different spray distances has been investigated. The spurt duration for all the experiments in this section is set as 40 ms which resembles that used in the clinical surgery. Firstly, we display variations of surface temperature ( $T_s$ ) and surface heat flux ( $q$ ) in Fig. 8, surface heat transfer coefficient ( $h$ ) and the total heat extraction per unit area ( $Q$ ) in Fig. 9 as the function of time for one certain nozzle ( $d_N=0.96$  mm) under one certain distance ( $z=30$  mm) just to point out some critical parameters. As shown from these two figures,  $T_s$  first decreases quickly from the ambient temperature to about -20 °C, then followed by a slow change over a long period of time until to the minimum surface temperature ( $T_{s,min}$ ). After reaching  $T_{s,min}$ ,  $T_s$  begins to rise. This surface temperature variation shows same tendency as those in Aguilar's studies [10, 11]. However, the time needed for the first quick decrease of Fig. 8 is much less than those by others. The quick variation of  $T_s$  is attributed to the fast response of thin film thermocouple in our experiments. Correspondingly, the surface heat flux ( $q$ ) experiences a first quick increase to a peak value ( $q_{max}$ ) and a followed gradual decrease until to zero when  $T_s$  begins to rise. However, the surface heat transfer coefficient ( $h$ ) has a fluctuant stage after reaching the maximum value ( $h_{max}$ ), which is quite different from the variations of  $T_s$  and  $q$ . The total heat extraction per unit area ( $Q$ ) monotonically increases with time as expected until the cryogen on the surface evaporates completely (i. e.  $T_s$  begins to rise).

The variation of the minimum surface temperature ( $T_{s,min}$ ) with spray distance for different diameter nozzles is shown in Fig. 10. It can be seen that  $T_{s,min}$  monotonically increases and declines within the spray distance of 90 mm for the smallest diameter nozzle (i. e.  $d_N=0.48$  mm) and the largest diameter nozzle (i. e.  $d_N=1.75$  mm), while it firstly declines and then increases with the spray distance for the two medial diameter nozzles. Meanwhile, the minimum value of  $T_{s,min}$  for these two medial diameter nozzle emerges at the distance of about 30 mm.

Fig.11 shows the variation of the maximum surface heat flux ( $q_{max}$ ) with the spray distance for different diameter nozzles. The nozzle diameter has little effect on the trend of the variation of  $q_{max}$  with the distance. For all the nozzles,  $q_{max}$  firstly increases to the maximum value and then decreases with the spray distances. After reaching the maximum value,  $q_{max}$  decreases more rapidly with the smaller diameter nozzle. The distance for the maximum value of  $q_{max}$  is 30 mm except the largest diameter nozzle. However, the value of  $q_{max}$  is dependent on the nozzle diameter. For all the measured points, the larger diameter nozzle can produce the larger  $q_{max}$  due to the greater impact on the cooling surface depicted as in Fig. 4 and Fig.5. This finding conforms to those by Aguilar et al. [6, 7].

The variation of the maximum surface heat transfer coefficient ( $h_{max}$ ) with the spray distance for different diameter nozzles is displayed in Fig. 12. It's noticed that the four nozzles can be divided into two groups according to the performance of  $h_{max}$ . One includes the smaller diameter nozzles of 0.48 mm and 0.96mm, in which  $h_{max}$  monotonically decreases with the spray distance. The other one is those with the larger diameter of 1.21 mm and 1.75 mm, where  $h_{max}$  first increases, and then decreases with the spray distance. Additionally, the smallest diameter nozzle produces the largest value of  $h_{max}$  as the spray distance is very small (i. e.  $z=10$  mm) due to the much lower spray droplet temperature as seen in Fig. 6. On the contrary, the larger diameter nozzle generates higher value of  $h_{max}$  at the spray region of 30 mm to 90 mm due to the larger  $q_{max}$  depicted as Fig. 11.

### 3.4. Discussion on the selection of the nozzle

From the clinical standpoint to protect the epidermis from the nonspecific thermal injury by the absorption of the laser energy, CSC should do the best to remove the heat from the epidermis during one pulsed spray. As shown in Fig. 9, the effective cooling time is about 200 ms for the pray of 40 ms spurt duration. Although further prolonging the spurt duration may slightly increase the effective cooling time, it will also increase the thickness of the liquid cryogen film on the cooling surface and will not further decrease the surface temperature, which has a negligible impact on both  $q$  and  $Q$  [11]. Therefore, we propose the total heat extraction per unit area within the first 200 ms ( $Q_{200}$ ) as a criterion to evaluate the cooling efficiency of CSC.

Fig.13 shows the variation of  $Q_{200}$  with the nozzle diameter under four different spray distances. It's noticed that  $Q_{200}$  monotonically decreases with the increment of the nozzle diameter under the very small spray distance of 10 mm, which indicates that it's better to use the smaller diameter nozzle for the spray at very small spray distance. The monotonic decrease of  $Q_{200}$  attributes to the large momentum droplets even for the smallest diameter nozzle in this very small spray distance as seen in Fig. 4 and Fig.5. The large momentum sprays may induce a large number of droplets to rebound from the surface. Increasing the nozzle diameter will further generate higher momentum droplets and enhance the bounce, which results in further decrease of  $Q_{200}$ . For the other three spray distances ( $z=30$  mm, 50 mm and 90 mm),  $Q_{200}$  firstly increases and then decreases with increasing the nozzle diameter. The first increase of  $Q_{200}$  mainly attributes to that the larger diameter nozzle can produce much larger  $q_{max}$  for the long spray distance as seen in Fig. 11. The points that the maximum value of  $Q_{200}$  happens are 0.96 mm for the spray distance of 30 mm and 50 mm, 1.21 mm for 90 mm, respectively. This early increase of  $Q_{200}$  with nozzle diameter at longer spray distance suggests that one may appropriately use the large diameter nozzle in order to enhance the heat removal.

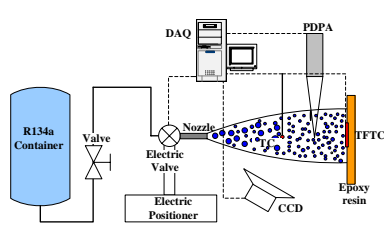


Figure 1 Schematic of the experimental system.

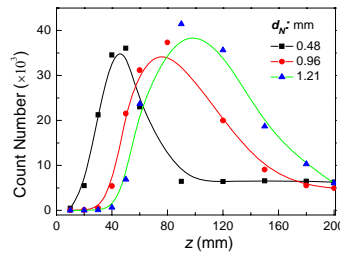


Figure 2 Variation of centerline droplets number by PDPA measurement along the spray axial distance for three nozzles.

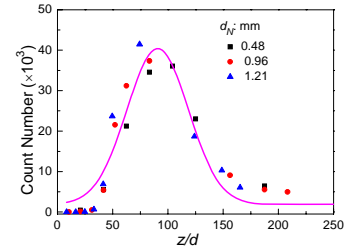


Figure 3 Droplets number variations with the dimensionless spray axial distance.

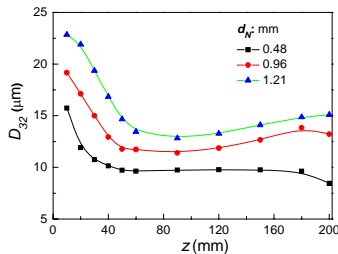


Figure 4 Variation of the centerline average droplet diameter ( $D_{32}$ ) with the axial distance for different diameter nozzles.

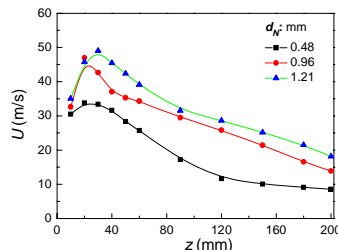


Figure 5 Variation of the centerline average droplet axial velocity with the axial distance for different diameter nozzles.

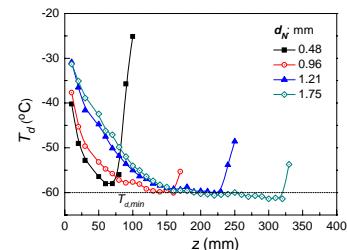
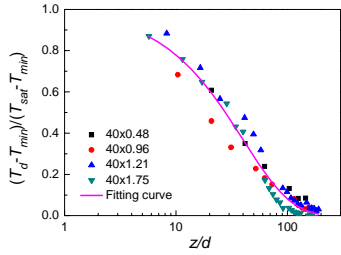
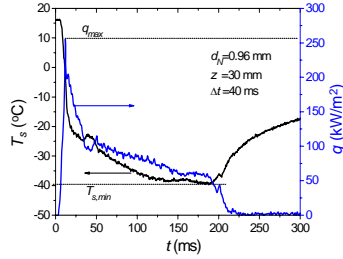


Figure 6 Variation of the centerline average droplet temperature with the axial distance for different diameter nozzles.



**Figure 7** Variation of the center-line average droplet non-dimensional temperature with the axial non-dimensional distance.



**Figure 8** Variations of surface temperature and surface heat flux as function of time.

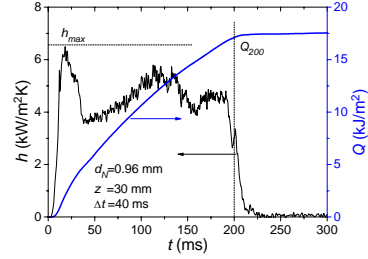


**Figure 9** Variations of surface heat transfer coefficient and total heat extraction per unit area as function of time.

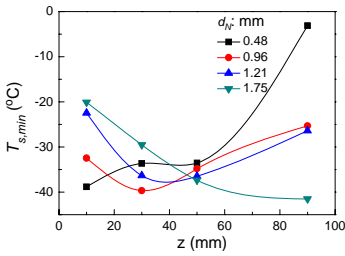


**Figure 10** Variation of the minimum surface temperature with the spray distance for different diameter nozzles.

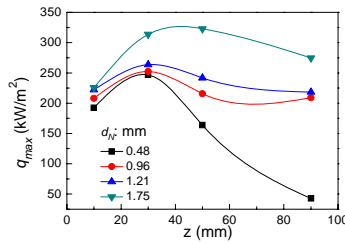


**Figure 11** Variation of the maximum surface heat flux with the spray distance for different diameter nozzles.

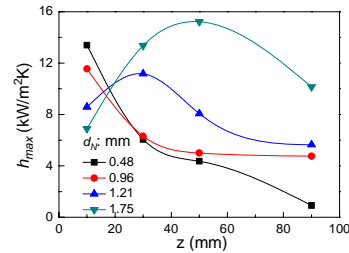


**Figure 12** Variation of the maximum surface heat transfer coefficient with the spray distance for different diameter nozzles.

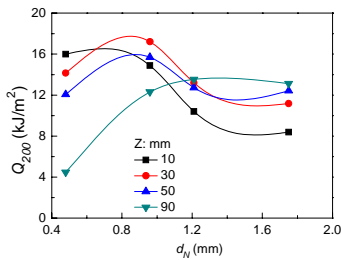


**Figure 13** Variation of the effective heat extraction with the nozzle diameter for under different spray distances.

#### 4. Summary and Conclusions

Experiments have been conducted to investigate the spray characteristics by the PDPA and the rapid variation of the surface temperature during CSC by the fast-response thin film thermocouple. The Duhamel's theorem was employed to calculate the surface heat flux ( $q$ ) and heat transfer coefficient ( $h$ ). The paper presents a systematic parametric study to illustrate the effect of the nozzle diameter on the spray characteristics and surface heat transfer dynamics and proposes a criterion to evaluate the cooling efficiency of the nozzles under different spray distances. The main findings can be summarized as following:

- 1) Smaller diameter nozzle has a better atomization capacity characterized by the shorter best atomized distance, lower average droplet diameter ( $D_{32}$ ) and average droplet velocity ( $U$ ).
- 2) The average droplet temperature ( $T_d$ ) in spray from the smaller diameter nozzle shows a faster exponential decay and a shorter distance for the minimum temperature ( $T_{d,min}$ ). However, the value of  $T_{d,min}$  for all the nozzles is nearly the same of about  $-60$  °C, and all  $T_d$  in the decay stage can be correlated by one exponential equation after the normalization.
- 3) The surface temperature ( $T_s$ ), heat flux ( $q$ ) and heat transfer coefficient ( $h$ ) show a strong dynamics with

time. Smaller diameter nozzle produces lower  $T_{s,min}$  and higher  $h_{max}$  at the very short spray distance, while larger diameter nozzle always produces higher  $q_{max}$ , especially for the long spray distance due to the impact of greater droplets on the cooling surface.

- 4) Based on the criterion that the total heat extraction ( $Q_{200}$ ) within the first 200 ms, it's recommended to choose smaller diameter nozzle at the very short spray distance ( $z=10$  mm) for the use in CSC, while to choose medial diameter nozzle at the spray distance of 30 mm. Further prolonging the spray distance, one should use the nozzles with larger diameter to guarantee the cooling efficiency.

### Acknowledgements

This work was supported by Chang Jiang Scholars Program of the Ministry of Education of China and Li KaShing Foundation of Hong Kong (G.-X. Wang, 2006-2009) and the Fundamental Research Funds for the Central University (2011jdhz35). Also, we acknowledge the financial support from the State Key Laboratory of Multiphase Flow in Power Engineering, Xi'an Jiaotong University.

### References

- [1] Esterly, N. B., *Current Problem in Dermatology* 7-3:69-107 (1996).
- [2] Lanigan, S. W., Cotterill, J. A., *British Journal of Dermatology* 121-2: 209-215 (1989).
- [3] Anderson, R. R., Parrish, J. A., *Science* 220-4596: 524-527 (1983).
- [4] Chang, C. J., Nelson, J. S., *Dermatologic Surgery* 25-10: 766-771(1999).
- [5] Nelson, J. S., Milner, T. E., Anvari, B., Tanenbaum, B. S., Kimel, S., Svaasand, L. O., Jacques, S. L., *Archives of Dermatology* 131-6: 695-700 (1995).
- [6] Aguilar, G., Verkruysse, W., Majaron, B., Svaasand, L. O., Lavernia, E. J., Nelson, J. S., Nelson, *IEEE Journal of Selected Topics in Quantum Electronics* 7-6: 1013-1021 (2001).
- [7] Aguilar, G., Majaron, B., Pope, K., Svaasand, L. O., Lavernia, E. J., Nelson, J. S., *Lasers Surgery and Medicine* 28-2: 113-120 (2001)
- [8] Aguilar, G., Wang, G. X., Nelson, J. S., *Lasers Surgery and Medicine* 32-2: 152-159 (2003).
- [9] Aguilar, G., Vu, H., Nelson, J. S., *Physics in Medicine and Biology* 49-10: N147-N153 (2004).
- [10] Wang, G. X., Aguilar, G., Nelson, J. S., *ASME National Heat Transfer Conference*, Las Vegas, NV, July 21-23, 2003.
- [11] Aguilar, G., Wang, G. X., Nelson, J. S., *Physics in Medicine and Biology* 48-14: 2169-2181 (2003).
- [12] Pikkula, B. M., Torres, J. H., Tunnel, J. W., Anvari, B., *Lasers in Surgery and Medicine*, 28-2: 103-112 (2001)
- [13] Jennifer, K., Chen, M. D., PedramGhasri, Aguilar, G., Anne Margreet van Drooge, Albert Wolkerstorfer, Kristen, M., Kelly, M. D., *Journal of the American Academy Dermatology*, 10.1016/j.jaad. 2011.11.938 (in Press)
- [14] Aguilar, G., Majaron, B., Verkruysse, W., *International Journal of Heat and Mass transfer*, 44-17:3201-3211 (2001).
- [15] Torres, J. H., Anvari, B., Tanenbaum, B.S., Milner, T. E., Yu, J. C., nelson, J. S., *Conference on Lasers in Surgery - Advanced Characterization, Therapeutic, and Systems*, SAN JOSE, CA, JAN 23-24, 1999.
- [16] Zhou, Z. F., Wu, W. T., Wang, G. X., Chen, B., Wang, Y. S., Gong, Z., *CIESC Journal* 62-11: 2691-2695(2011). (in Chinese)
- [17] Franco, W., Liu, J., Wang, G. X., Nelson, J. S., Aguilar, G., *Physics in Medicine and Biology* 50-2: 387-397 (2005).
- [18] Zhou, Z. F., Chen, B., Wang, Y. S., Guo, L. J., Wang, G. X., *Applied Thermal Engineering*, 39: 29-36 (2012).
- [19] Yildiz, D., van Beeck, J., Riethmuller, M. L., *Particle & Particle Systems Characterization* 21-5: 390-402 (2004).
- [20] Vu, H., Garcia-Valladares, O., Aguilar, G., *International Journal of Heat and Mass Transfer*, 51-23: 5721-5731 (2008).
- [21] Zhou, Z. F., Wu, W. T., Wang, G.-X., Zheng, G., Chen, B., Wang, Y. S., Guo, L. J., *ASME International Mechanical Engineering Congress & Exposure*, Denver, Colorado, November 11-17, 2011.
- [22] Yildiz, D., Rambaud, P., Van Beeck, J. P. J. A., Buchlin, J.-M., *ICLASS 2003-9th International Conference on Liquid Atomization and Spray Systems*, Sorrento, Italy, 2003.